Optical property study of FePt-C nanocomposite thin film for heat-assisted magnetic recording

Z. H. Cen*, B. X. Xu, J. F. Hu, J. M. Li, K. M. Cher, Y. T. Toh, K. D. Ye, and J. Zhang

Data Storage Institute, Agency for Science, Technology and Research (A-STAR), 117608 Singapore
*cen_zhanhong@dsi.a-star.edu.sg

Abstract: Optical properties of the FePt-C nanocomposite thin film that was synthesized by sputtering with MgO/NiTa underlayer on glass substrate have been determined by an approach combining spectroscopic ellipsometry and transmission over the wavelength range of 380 – 1700 nm. It was observed that the refractive index is larger than the extinction coefficient, indicating that free electron absorption is not the dominant optical transition in the FePt-C thin film. Compared with FePt thin film, the FePt-C thin film has smaller optical constants, which lead to better optical performance including smaller optical spot on recording media and higher transducer efficiency for heat assisted magnetic recording.

OCIS codes: (240.2130) Ellipsometry and polarimetry; (160.4236) Nanomaterials; (240.6680) Surface plasmons; (050.1755) Computational electromagnetic methods.

References and links

1. T. Suzuki, H. Muraoka, Y. Nakamura, and K. Ouchi, "Design and recording properties of FePt perpendicular media," IEEE Trans. Magn. **39**(2), 691–696 (2003).
2. J. S. Chen, J. F. Hu, B. C. Lim, Y. F. Ding, G. M. Chow, and G. Ju, "Development of $L1_0$ FePt:C (001) thin films with high coercivity and small grain size for ultra-high-density magnetic recording media," IEEE Trans. Magn. **45**(2), 839–844 (2009).
3. K. F. Dong, H. H. Li, Y. G. Peng, G. Ju, G. M. Chow, and J. S. Chen, "Well-isolated $L1_0$ FePt-SiN_x-C nanocomposite films with large coercivity and small grain size," J. Appl. Phys. **111**(7), 07A308 (2012).
4. J. S. Chen, B. C. Lim, Y. F. Ding, J. F. Hu, G. M. Chow, and G. Ju, "Granular $L1_0$ FePt-X (X=C, TiO_2, Ta_2O_5) (001) nanocomposite films with small grain size for high density magnetic recording," J. Appl. Phys. **105**(7), 07B702 (2009).
5. S. D. Granz and M. H. Kryder, "Granular $L1_0$ FePt (001) thin films for Heat Assisted Magnetic Recording," J. Magn. Magn. Mater. **324**(3), 287–294 (2012).
6. T. Song, T. J. Zhou, C. L. Chen, and H. Gong, "XPS study of thermal effects on FePt and FePtAg nanoparticles," IEEE Trans. Magn. **41**(10), 3367–3369 (2005).
7. M. H. Kryder, E. C. Gage, T. W. McDaniel, W. A. Challener, R. E. Rottmayer, G. P. Ju, Y. T. Hsia, and M. F. Erden, "Heat Assisted Magnetic Recording," Proc. IEEE **96**(11), 1810–1835 (2008).
8. S. J. Lee, A. C. C. Yu, C. C. H. Lo, and M. Fan, "Optical properties of monodispersive FePt nanoparticle films," Phys. Status Solidi **201**(13), 3031–3036 (2004) (a).
9. S. L. Lee, C. C. H. Lo, A. C. C. Yu, and M. Fan, "Spectroscopic ellipsometry study of FePt nanoparticle films," Phys. Status Solidi **203**(15), 3801–3804 (2006) (a).
10. J. F. Hu, J. S. Chen, B. C. Lim, and B. Liu, "Underlayer diffusion-induced enhancement of coercivity in high anisotropy FePt thin films," J. Magn. Magn. Mater. **320**(22), 3068–3070 (2008).
11. G. K. Pribil, B. Johs, and N. J. Ianno, "Dielectric function of thin metal films by combined in situ transmission ellipsometry and intensity measurements," Thin Solid Films **455–456**, 443–449 (2004).
12. Y. H. Yang and J. R. Abelson, "Spectroscopic ellipsometry of thin films on transparent substrates: A formalism for data interpretation," J. Vac. Sci. Technol. A **13**(3), 1145–1149 (1995).
13. B. Harbecke, "Coherent and incoherent reflection and transmission of multilayer structures," Appl. Phys. B **39**(3), 165–170 (1986).
14. N. Zhou, E. C. Kinzel, and X. F. Xu, "Nanoscale ridge aperture as near-field transducer for heat-assisted magnetic recording," Appl. Opt. **50**(31), G42–G46 (2011).
15. D. A. G. Bruggeman, "Calculation of various physics constants in heterogenous substances I. Dielectricity constants and conductivity of mixed bodies from isotropic substances," Ann. Phys. (Leipzig) **24**(7), 636–664 (1935).
16. S. Logothetidis, M. Gioti, S. Lousinian, and S. Fotiadou, "Haemocompatibility studies on carbon-based thin films by ellipsometry," Thin Solid Films **482**(1-2), 126–132 (2005).

#181627 - $15.00 USD Received 12 Dec 2012; revised 10 Mar 2013; accepted 12 Mar 2013; published 15 Apr 2013

17. E. S. Kooij, H. Wormeester, E. A. M. Brouwer, E. van Vroonhoven, A. van Silfhout, and B. Poelsema, "Optical characterization of thin colloidal gold films by spectroscopic ellipsometry," Langmuir **18**(11), 4401–4413 (2002).
18. C. Q. Sun, "Size dependence of nanostructures: Impact of bond order deficiency," Prog. Solid State Chem. **35**(1), 1–159 (2007).
19. B. X. Xu, Z. H. Cen, Y. T. Toh, J. M. Li, K. D. Ye, and J. Zhang, "Efficiency analysis of near field optical transducer used in heat-assisted magnetic recording," IEEE Trans. Magn. (to be published).

1. Introduction

FePt nanocomposite thin films with good $L1_0$ FePt (100) texture have been regarded as one of the most promising candidates for ultra-high density magnetic recording media, because of their large magnetocrystalline anisotropy, K_u (7×10^7 erg/cm^3) that can suppress superparamagnetism at room temperature at a small particle size even below 10 nm [1–3]. Up till now, much study has been focused on the material synthesis and its structural and magnetic properties [4,5]. It has been demonstrated that a monolayer of $L1_0$ FePt nanoparticles with good magnetic properties embedded in a nonmagnetic material matrix has been successfully fabricated by chemical synthesis method and sputtering technique, separately [3–6]. However, existing magnetic recording heads cannot provide a magnetic field large enough to write FePt nanocomposite thin films with such high K_u using conventional writing schemes. To address this problem, heat-assisted magnetic recording (HAMR) has been proposed [7]. In HAMR, the recording medium is heated up to its Curie temperature by light locally and temporarily to lower the magnetic anisotropy during the recording process. Because of the interaction between light and recording media in HAMR, optical properties of FePt nanocomposite thin films are indispensable for HAMR system design and modeling.

Unlike the structural and magnetic properties of FePt nanocomposite thin films, its optical properties have seldom been studied [8,9]. A chemically synthesized FePt nanoparticle thin film with coupling layers on SiO_2/Si substrate has been characterized by spectroscopic ellipsometry (SE), and it was shown that optical properties of the FePt nanoparticle film are different from those of the bulk and thin film counterparts [8]. To the best of our knowledge, optical properties of FePt nanocomposite films fabricated by sputtering that is preferred for industrial manufacturing have not been fully investigated yet. In addition, optical properties of FePt nanocomposite films could strongly depend on the fabrication condition and technique [9]. In this paper, study of optical properties of a FePt nanocomposite thin film doped with C (FePt-C) is reported. The thin film with MgO/NiTa underlayer on glass substrate was fabricated by sputtering. Due to the transparent substrate used in samples, SE together with transmission was employed to determine optical functions (i.e., refractive index n and extinction coefficient k as functions of wavelength) of the FePt-C thin film over the visible and near-infrared (near-IR) spectrum. Using the extracted FePt-C optical constants for the recording layer in a HAMR system, optical field distribution in the recording layer was simulated by finite-difference time-domain (FDTD) method. By comparing with the FePt film without doping C, it is shown that doping C into FePt thin film changes the thin film optical properties, which results in better optical performance as the HAMR recording layer.

2. Experimental details and modeling

The sample layer structure is FePt-C/MgO intermediate layer/NiTa seed layer/glass substrate, as shown in Fig. 1(a). The NiTa layer can help the subsequent deposition of the crystalline MgO layer, besides facilitating heating the glass substrate uniformly in sample preparation. In order to avoid warp in the disk due to stress unbalance at high temperature during FePt-C deposition, each side of the substrate was coated with a NiTa layer. The MgO layer provides appropriate crystal lattice to epitaxially grow highly chemically ordered $L1_0$ FePt-C films with perpendicular anisotropy. Meanwhile, the MgO layer can block diffusion of the NiTa layer into the magnetic layer. The whole sample was prepared in a high vacuum magnetron sputtering system. NiTa and MgO layers were deposited at room temperature, while the FePt-

#181627 - $15.00 USD Received 12 Dec 2012; revised 10 Mar 2013; accepted 12 Mar 2013; published 15 Apr 2013

C layer was deposited at high temperature of 600 °C. Cosputtering of FePt alloy and C targets was used to deposit the FePt-C film. The volume fraction of C in the FePt-C thin film was designed to be 50%. Figure 1(b) shows a cross-section transmission electron microscopy (TEM) image of the FePt-C thin film. FePt nanoparticles with diameters of around 15 nm and heights of around 9.1 nm embedded in a C matrix can be observed in the TEM image. For comparison, a FePt thin film without doping C in the same layer structure was prepared at the same fabrication condition as a reference. The FePt thin film fabricated at high temperature is composed of large $L1_0$ FePt grains with diameters of around 50 nm that can be evidenced in atomic force microscopy(AFM) images (not shown here), and similar results have been reported in previous studies [10]. Moreover, control samples with successive layer structures (NiTa/Glass/NiTa & MgO/NiTa/Glass/NiTa) were also prepared at the same conditions.

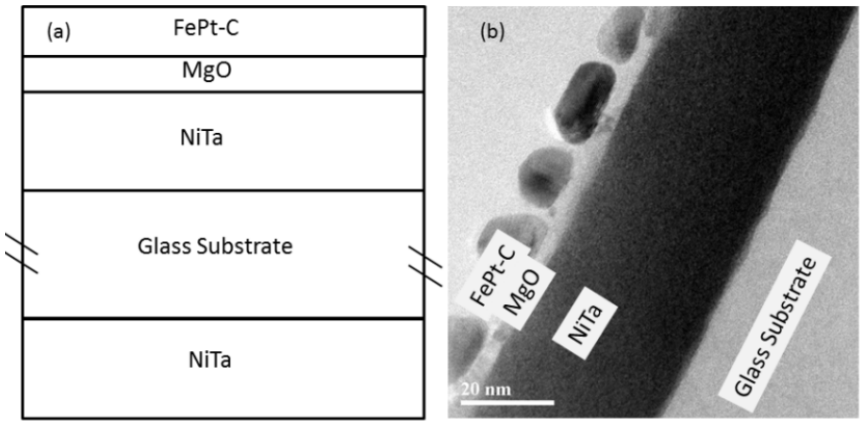

Fig. 1. (a) A schematic of the FePt-C sample layer structure. (b) Cross-sectional TEM image of the FePt-C thin film.

SE measurement was conducted on samples at room temperature over a wavelength range from 380 to 1700 nm with a step of 5 nm at 3 incident angles (i.e., 65°, 70° and 75°), using a variable angle spectroscopic ellipsometer. Transmission (T) at normal incidence was also measured on the samples over the same wavelength range. Simultaneous analysis of the data obtained from both measurement techniques (i.e., SE and T) can improve accuracy of the extracted SE results, because correlation effect between thickness and optical constants of absorbing thin films can be alleviated [11]. An optical multilayer model consisting of seven phases (i.e., Ambient/FePt-C/MgO/NiTa/Glass Substrate/NiTa/Ambient) as shown in Fig. 1(a) was used in spectral analysis of the measured ellipsometric angles (i.e., Ψ and Δ) and the transmission intensity. Optical functions of the NiTa and MgO layers as well as those of the glass substrate were measured from the corresponding control samples and a clean glass substrate, respectively. Thicknesses of the NiTa and MgO layers were determined to be 34.8 and 6.6 nm. The glass substrate thickness was measured by Vernier caliper, and it is 635 μm. The thicknesses of the NiTa and MgO layers and the substrate were fixed during spectral analysis for the FePt-C sample. Surface roughness of the FePt-C film, whose root mean square roughness R_q is 0.9 nm in this study, is not included in the optical model here. As a result, the retrieved optical constants are effective optical properties of the FePt-C film, and are not exactly reflective of all detailed thin film structures.

In experiment, it was observed that the effect of reflection from the glass substrate backside on SE is obvious due to the comparatively thin NiTa layer grown in our samples. An incoherent treatment was employed for the light propagation within the glass substrate, because the glass substrate thickness exceeds the light coherent length [12]. By incorporating this incoherent light propagation with the coherent light propagation in other thin layers in the optical multilayer model, the Fresnel reflection coefficients (r) can be calculated for the light

#181627 - $15.00 USD Received 12 Dec 2012; revised 10 Mar 2013; accepted 12 Mar 2013; published 15 Apr 2013

component parallel (*p*) or perpendicular (*s*) to the incident plane. Following the basic ellipsometry equation

$$\tan(\Psi)e^{-i\Delta} = \frac{r_p}{r_s}, \tag{1}$$

ellipsometric angles can be expressed in terms of the optical constants and the thickness of the FePt-C layer. Given an initial value for the FePt-C layer thickness, optical functions of the FePt-C layer can be obtained from fitting the SE spectra. In the present study, a point-by-point fitting approach was used, where a separate regression analysis to achieve minimal SE mean-square error (MSE) was carried out on the SE data of 3 incident angles at each wavelength using a pair of initial values for FePt-C optical constants. In order to obtain continuous optical functions without unphysical abrupt changes, averages of *n* and *k* values determined at three previous wavelengths were used as *n* and *k* initial values for the next wavelength. Using a given FePt-C layer thickness and the corresponding optical functions determined by SE, transmission can be calculated based on the optical multilayer model [13]. By freely varying the FePt-C layer thickness, the transmission MSE can be minimized, which is given by

$$MSE^T = \frac{1}{N}\sum_{i=1}^{N}\left(\frac{T_i^{cal} - T_i^{\exp}}{\delta T_i^{\exp}}\right)^2, \tag{2}$$

where N is the number of data points, T^{cal} and T^{exp} are the calculated and measured transmission intensity, and δ is the experimental data standard deviation. Using this method, spectral fittings of the SE and T data were carried out simultaneously, which yielded optical functions and thickness of the FePt-C thin film. Similar spectral fitting process was also carried out for the FePt reference sample.

In order to evaluate optical performance of the FePt-C thin film as the recording layer in HAMR systems, the extracted FePt-C and FePt optical functions were employed for the recording layer in FDTD simulation of a simple HAMR system. In the HAMR system, a C-shape aperture transducer in gold (Au) film on a glass substrate and the recording medium were included in simulation [14]. A light source at 780 nm with a Gaussian intensity distribution normally shining on the Au film was used to excite plasmons of the transducer. The Gaussian beam is focused to a diameter of 2 μm by a lens with numerical aperture (NA) of 0.33. The field magnitude of the light source was set at 1 V/m. The simulation boundaries were set to be perfectly matched layers to absorb the electromagnetic energy incident upon them. The whole FDTD simulation was conducted by using commercial software, Lumerical FDTD Solutions.

3. Results and discussion

The spectral fittings for the FePt-C and FePt samples are shown in Fig. 2. As can be seen in Fig. 2(a), the SE spectra are well fitted by the point-by-point fitting approach, which have an average SE MSE around 1.5 for all fitting wavelengths. In addition, a good fitting with transmission MSE smaller than 1 is also achieved in the transmission spectra over the whole measured wavelength range as shown in Fig. 2(b). The thickness of the FePt-C thin film yielded from the fittings is 7.8 nm, which agrees with the TEM measurement result. The slight difference of the FePt-C film thickness from the height of FePt nanoparticles in the FePt-C film revealed in Fig. 1(b) could result from the FePt-C film roughness, and the FePt-C film thickness yielded by the optical model shown in Fig. 1(a) is an average thickness.

#181627 - $15.00 USD Received 12 Dec 2012; revised 10 Mar 2013; accepted 12 Mar 2013; published 15 Apr 2013

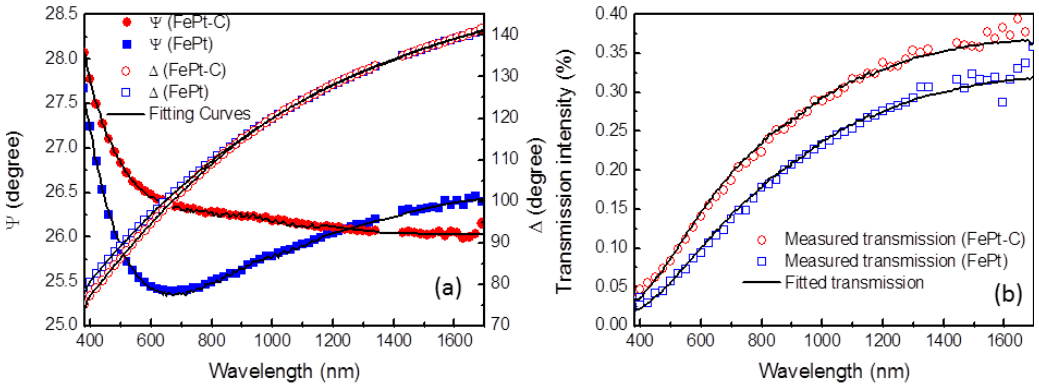

Fig. 2. (a) SE and (b) transmission spectral fittings for FePt-C and FePt thin films.

Figure 3 shows the yielded optical functions of the FePt-C thin film, as well as those of the FePt thin film for comparison. There is no prominent peak shown in the FePt-C optical functions. The refractive index of the FePt-C thin film increases with wavelength, while the corresponding extinction coefficient is around 1.75 over the wavelength range between 380 and 1300 nm, but increases with wavelength at the near-IR wavelengths longer than 1300 nm, which could be attributed to free electron absorption. However, the FePt-C refractive index is larger than the extinction coefficient at near-IR wavelengths, which is different from metallic characteristics. In addition, a similar result between refractive indexes and extinction coefficients at near-IR wavelengths can also be observed for the FePt thin film in the present study, showing that C with small extinction coefficients in the FePt-C film is not the only cause of the experimental result. Therefore, the dielectric-like FePt-C optical functions at near-IR wavelengths indicate that free electron absorption does not dominate FePt-C optical transitions. And it can be explained by the intrinsic scattering inside FePt nanoparticles, such as scattering by FePt crystal defects, and the scattering on the surfaces of FePt nanoparticles [9], which would increase with decreasing the nanoparticle size.

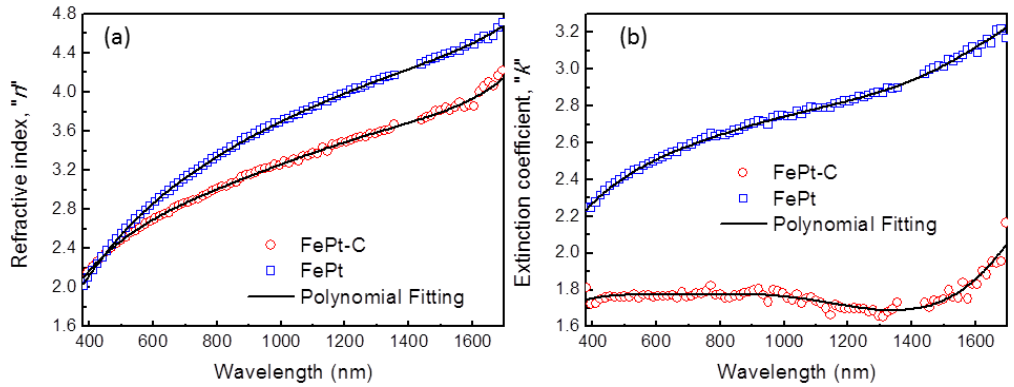

Fig. 3. (a) Refractive index and (b) extinction coefficient of FePt-C and FePt thin films as functions of wavelength. Smoothing optical functions using polynomial fitting is given also.

By comparing the optical functions of FePt-C and FePt thin films, significant decrease in optical constants, particularly in extinction coefficient, can be observed after doping C. According to the effective medium approximation theory [15], inclusion of C into FePt can reduce the thin film effective optical constants, because C has lower optical constants with respect to FePt [16]. On the other hand, because of the increasing importance of the atom layer on nanoparticle surface and the limited particle size relative to the electron mean free path [17,18], FePt nanoparticles could have smaller optical constants as compared with the

#181627 - $15.00 USD Received 12 Dec 2012; revised 10 Mar 2013; accepted 12 Mar 2013; published 15 Apr 2013

bulk counterpart [9]. As a result, the FePt-C thin film shows optical constants distinct from those of the FePt thin film. Moreover, they can be tuned by adjusting the volume fraction ratio between FePt nanoparticles and the C matrix in the FePt-C film.

In order to employ the extracted optical properties of FePt-C and FePt thin films in HAMR system simulation, the FePt-C and FePt optical functions were smoothed by polynomial fitting as shown in Fig. 3. The simulation model of the HAMR system with the recording medium is shown in Fig. 4(a), and the structure of the C-aperture transducer in the HAMR system is given in Fig. 4(b). The recording medium consists of a 10 nm recording layer, a 6 nm MgO layer, a 6 nm NiTa layer, and a 50 nm Au layer on a glass substrate. Here, the Au layer acts as a heat sink layer to improve the medium thermal property in practical case. FePt-C and FePt were used as the recording layer, respectively. The polarization of the incident light is along y direction. A 4 nm air gap between the transducer and the top surface of the recording medium was set in the simulation. Optical constants of the used materials at wavelength of 780 nm are listed in Table 1.

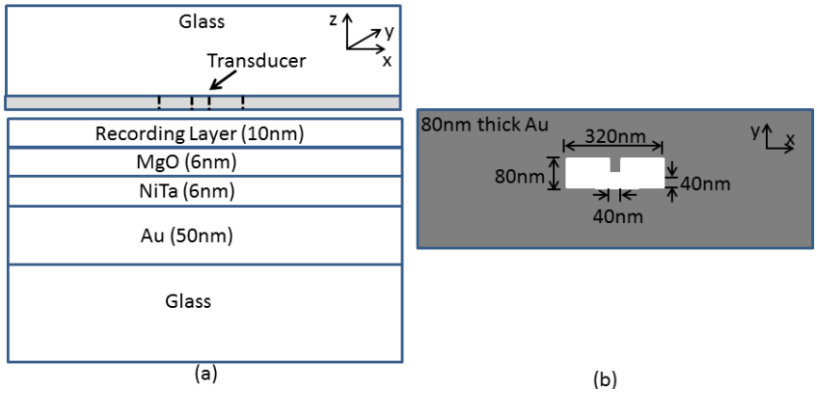

Fig. 4. (a) Simulation model of HAMR system. (b) Structure of C-aperture transducer.

Table 1. Optical constants (at 780 nm) of materials used in FDTD simulation

Material	Optical constant
Au	0.15 + i4.76
FePt	3.30 + i2.63
FePt-C	2.98 + i1.78
MgO	1.60
NiTa	4.21 + i3.76
Glass substrate	1.45

Figure 5(a) shows the electric field intensity distribution on the top surface of the recording layer for the FePt-C and FePt cases, respectively. Similar optical spots with close values of maximum field enhancement were obtained in both cases. The optical spot size (full width at half maximum, FWHM) along x direction is nearly the same at 42.6 nm, while the spot size (FWHM) along y direction is 29 nm in the FePt-C case, which is 1 nm smaller than that in the FePt case. Although the difference of the optical spot size along the C-aperture ridge (i.e. along y direction) is not prominent, which is just close to the simulation mesh size (1 nm), it indicates that the propagation length of the surface plasmon along the Au/air interface is affected by the recording layer [14], and it is shorter when the optical constants of the recording layer are smaller.

#181627 - $15.00 USD Received 12 Dec 2012; revised 10 Mar 2013; accepted 12 Mar 2013; published 15 Apr 2013

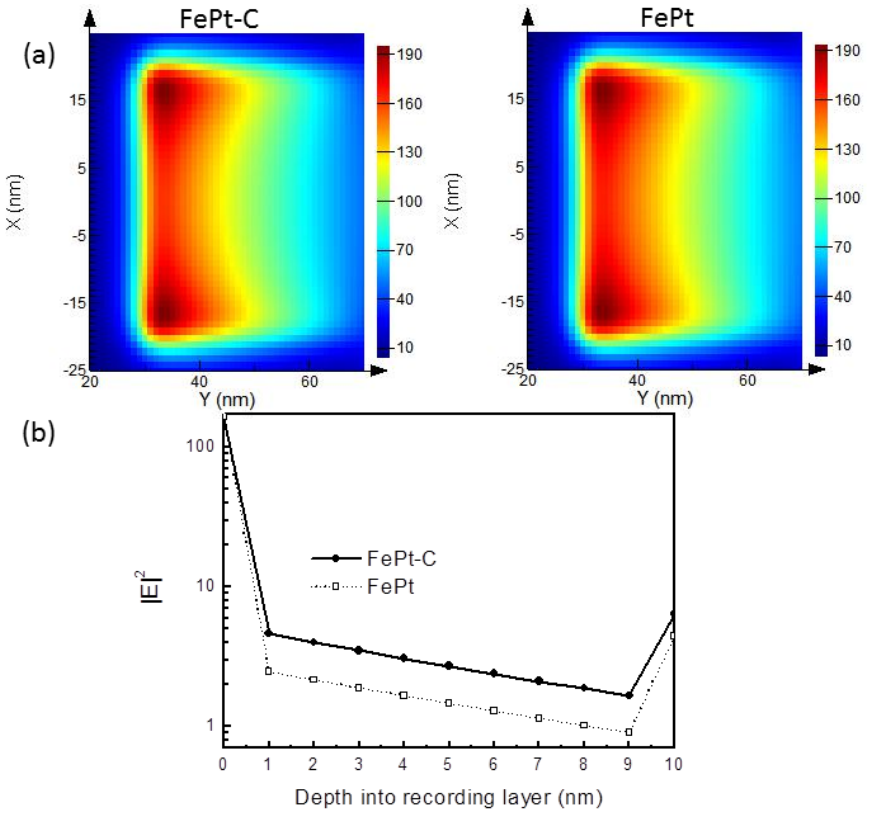

Fig. 5. (a) Electric field intensity distribution on the recording layer top surface in FePt-C and FePt cases. (b) Electric field intensity distribution in recording layer.

The transducer efficiency in this study is defined as a ratio of the power absorbed by the recording layer within a volume of 50 × 50 × 10 nm^3 to the incident power of the light source. It is found that the efficiency in the FePt-C case is 10% higher than that in the FePt case (FePt-C: 0.4%, FePt: 0.36%). In Fig. 5(b), the optical intensity ($|E|^2$) distributions in the recording layer underneath the center of the C-aperture ridge edge are presented for both cases. Note that due to the light resonance in the non-absorbing MgO layer, the electric field intensity in the MgO layer is larger than that in the recording layer. And because of simulation of the electric field intensity at the recording layer interface (depth of 0 and 10 nm in Fig. 5(b)), there is an abrupt change at the mesh point closest to the interface (depth of 1 and 9 nm in Fig. 5(b)) in the simulated electric field distribution. It can be seen that the electric field intensity is reduced significantly in the recording layer, which can be explained in terms of the equations for the electric field across the interface between air gap and recording layer:

$$E_{x,y}^{recordinglayer} = E_{x,y}^{air} \tag{3}$$

$$\frac{E_z^{recordinglayer}}{E_z^{air}} = \frac{1}{|n+ik|^2}, \tag{4}$$

where $E_{x,y}$ is the electric field component along x or y direction, E_z is the component along z direction, while n and k are optical constants of the recording layer [19]. The major component of surface plasmons generated by the C-aperture transducer is E_z [19]. Therefore, large reduction of electric field intensity in the recording layer occurred. Because the FePt-C thin film has smaller optical constants relative to the FePt thin film as shown in Fig. 3, E_z

#181627 - $15.00 USD Received 12 Dec 2012; revised 10 Mar 2013; accepted 12 Mar 2013; published 15 Apr 2013

intensity in the FePt-C film is larger than that in the FePt film. Furthermore, power absorption (A) in the recording layer can be related to the electric field by the following equation

$$A = 0.5real\left(-i\omega E \bullet D\right) = 0.5\omega\left|E\right|^2 imag\left(\varepsilon\right), \tag{5}$$

where ω is the frequency of the excitation light source, D is the electric displacement field, and *imag(ε)* is the imaginary part of the dielectric function of the recording layer that equals $2nk$. Therefore, the power absorption in the recording layer due to the electric field of different orthogonal direction can be written as:

$$A_{x,y} \propto \left|E_{x,y}^{recordinglayer}\right|^2 nk \propto \left|E_{x,y}^{air}\right|^2 nk \tag{6}$$

$$A_z \propto \left|E_z^{recordinglayer}\right|^2 nk \propto \frac{\left|E_z^{air}\right|^2 nk}{\left|n+ik\right|^4}. \tag{7}$$

The portion of the incident power absorbed within the recording layer volume fraction that is used to calculate the transducer efficiency is plotted in Fig. 6 for different electric field components in FePt-C and FePt cases, which can reflect the contributions of the electric field components to the transducer efficiency. Note that the absorbed power portions in Fig. 6 are normalized to the transducer efficiency in the FePt-C case for comparison. Although smaller optical constants of FePt-C thin film reduces the power absorption from the electric field components along x and y direction, the power absorption from the electric field component along z direction is remarkably enhanced in the FePt-C case as compared with the FePt case, as shown Fig. 6. In addition, more than 50% of the transducer efficiency in this study is generated by the electric field component along z direction, which determines the transducer efficiency. Therefore, a better transducer efficiency in the HAMR system can be achieved using FePt-C thin film as the recording layer.

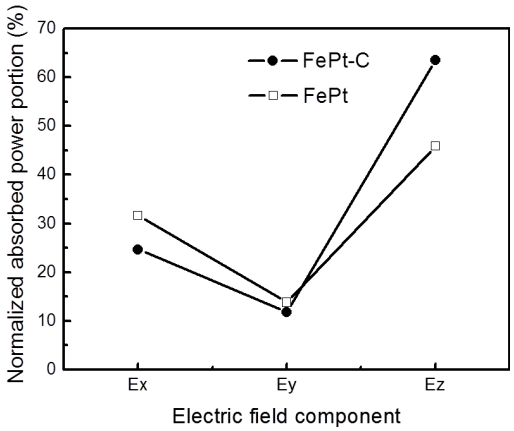

Fig. 6. Contributions of different electric filed components to transducer efficiency. All absorbed power portions are normalized to the transducer efficiency in the FePt-C case.

4. Summary

In summary, optical properties of the FePt-C nanocomposite thin film fabricated by sputtering with MgO/NiTa underlayer on glass substrate have been studied using SE and transmission. The FePt-C thin film have dielectric-like optical functions, where refractive index is larger than extinction coefficient at near-IR wavelengths, indicating that free electron absorption is not the dominant optical transition in FePt-C. As compared with the FePt thin film, significant reduction in optical constants can be observed in the FePt-C thin film. The extracted optical

#181627 - $15.00 USD Received 12 Dec 2012; revised 10 Mar 2013; accepted 12 Mar 2013; published 15 Apr 2013

constants were used for the recording layer in FDTD simulation of a HAMR system. Better HAMR optical performance including smaller optical spot size and higher transducer efficiency can be obtained in the case of FePt-C film as compared with the case of FePt film, and it is owed to the smaller optical constants of the FePt-C thin film. Results in this study show that besides the widely studied improvement in magnetic and thermal properties, doping C into FePt to fabricate FePt-C nanocomposite thin film can achieve better HAMR optical performance.

#181627 - $15.00 USD Received 12 Dec 2012; revised 10 Mar 2013; accepted 12 Mar 2013; published 15 Apr 2013